Unidirectional soliton flows in $\mathcal{PT}$-symmetric potentials

U. Al Khawaja,[1] S. M. Al-Marzoug,[2,3] H. Bahlouli,[2,3] and Yuri S. Kivshar[4]

[1]*Physics Department, United Arab Emirates University, P. O. Box 15551, Al-Ain, United Arab Emirates*

[2]*Physics Department, King Fahd University of Petroleum and Minerals, Dhahran 31261, Saudi Arabia*

[3]*Saudi Center for Theoretical Physics, Dhahran 31261, Saudi Arabia*

[4]*Nonlinear Physics Center, Research School of Physics and Engineering, Australian National University, Canberra ACT 0200, Australia*

(Received 30 May 2013; revised manuscript received 11 July 2013; published 19 August 2013)

We study the soliton scattering by parity-time- (PT) symmetric potentials and demonstrate that, for a certain range of parameters, both single and multiple soliton scattering exhibit almost perfect unidirectional flow. We employ direct numerical simulations of the corresponding nonlinear Schrödinger equation combined with the analysis of the effective equations derived by the collective-coordinate approach and reveal that the physical mechanism behind this effect of the unidirectional scattering is related to the energy exchange between the soliton center of mass and its internal mode.

DOI: 10.1103/PhysRevA.88.023830 PACS number(s): 42.65.Tg, 05.45.Yv, 03.75.Lm, 05.30.Jp

I. INTRODUCTION

Quantum mechanics requires that every physical observable is associated with a real spectrum and, hence, it was postulated that all operators representing such physical values should be Hermitian. This axiom guarantees conservation of probability and also takes care of the unitary temporal evolution of the system. However, in the past decade considerable attention [1,2] has been paid to the formulation of a weaker version of the Hermitian axiom which still requires the spectrum to be real. In a series of papers by Bender *et al.* [1], it was shown that even non-Hermitian Hamiltonians can exhibit real spectra provided they satisfy both parity and time-reversal symmetry referred to as *a parity-time (PT) symmetry*. A one-dimensional Hamiltonian is PT symmetric when the corresponding potential fulfils the condition $V(x) = V^*(-x)$, where x is the spatial coordinate and the asterisk stands for a complex conjugation which requires that the real part of the potential is even while its imaginary part is an odd function of position x.

The concept of PT-symmetric potentials can be extended to nonlinear models, and a new class of localized modes was found to exist below the PT-symmetry-breaking transition [3]. Subsequently, nonlinear modes were also studied in different types of complex PT symmetric potentials [4,5]. The existence of periodically oscillating solitons in PT-symmetric nonlinear couplers with gain or loss were also predicted [6].

Recently, it was proposed that optics can provide a fertile ground where PT-related concepts can be realized and experimentally tested [2]. This is due to the fact that there is close similarity between the effective wave propagation equation and the Schrödinger equation from quantum mechanics where the role of potential in the Schrödinger equation is played by the refractive index in optics. Motivated by this connection, optical systems which exhibit PT symmetry have been formulated [2]. Given that the complex refractive index of an optical one-dimensional system can be written as $n(x) = n_R(x) + in_I(x)$, where $n_R(x)$ is the real part and $n_I(x)$ is the imaginary part of the refractive index, respectively, and x is the transverse coordinate, a PT-symmetric effective optical potential $n(x)$ can be realized by a suitable design for the distribution of gain and loss in the medium, $n_I(x)$. The PT symmetry condition will, in this case, be satisfied with the real part of the refractive index profile of the medium, $n_R(x)$, being even and the gain or loss profile, $n_I(x)$, being an odd function of coordinate x.

Reflection and transmission of solitons through scattering potentials represents an interesting problem, being of the fundamental interest in condensed matter physics and nonlinear optics. For instance, it was shown that a quantum reflection from barriers and wells has a resonant character, where the internal modes of solitons and local impurity modes are interacting [7]. The case when defects exhibit equal gain or loss coefficients with a specific type of PT symmetry is of great interest. In this paper, we study the soliton scattering through a PT-symmetric potential, both analytically and numerically. Recently, scattering of a broad soliton in a nonlinear lattice with a PT-symmetric defect has been considered [8], where amplification of the soliton during the process of scattering was studied numerically. More recently, unidirectional reflectionless flow was demonstrated experimentally near the spontaneous parity-time symmetry phase transition point [9]. Here we show that under special conditions we can have nonreciprocity in the soliton transmission or a unidirectional soliton flow of solitons giving rise to a diode-type transmission effect.

The paper is organized as follows. In Sec. II we introduce our model and formulate the problem. In Sec. III, we perform numerical simulations for the solitons scattering through a PT-symmetric potential. Section IV is devoted to the collective-coordinate analysis of the model. Section V concludes the paper by summarizing our major findings.

II. PROBLEM FORMULATION

We begin our study with the traditional normalized nonlinear Schrödinger (NLS) equation that includes a PT-symmetric potential,

$$i\frac{\partial\psi}{\partial t} + \frac{1}{2}\frac{\partial^2\psi}{\partial x^2} + [V(x) + iW(x)]\psi + |\psi|^2\psi = 0\,, \quad (1)$$

where

$$V(x) = V_0\,\mathrm{sech}^2(\alpha x), \quad W(x) = W_0\,x\,\mathrm{sech}^2(\alpha x), \quad (2)$$

and V_0 and W_0 are real-valued constants corresponding to the depth or amplitude of the real an imaginary parts of the potential, respectively. The real part of the potential $V(x)$, known as the Rosen-Morse potential, belongs to the class of reflectionless potentials. The inverse width α is typically equal to $\sqrt{|V_0|}$ to maintain the reflectionless property. It is clear that since $V(x)$ and $W(x)$ are even and odd function, respectively, the PT symmetry requirement is satisfied. It has been shown that solitons scattered by this potential exhibit sharp transition in the transport coefficients at a certain critical incident center-of-mass speed of the soliton [7,10]. Such a sharp transition is crucial to the existence of the unidirectional flow described in this paper. We have investigated the effect of other potential wells. For instance, we found that the sharp transition in the transport coefficients is absent for a square potential well and present for a Gaussian potential well. The unidirectional flow thus has indeed been seen with the latter but not the former potential.

Launching a bright soliton on the PT-symmetric potential given by Eq. (2), we describe the dynamics of the scattered soliton by Eq. (1). The transport coefficients can then be calculated for the two directions of incidence showing the unidirectional flow. In the following section, this effect will be shown by solving numerically Eq. (1). In Sec. IV, a collective coordinate approach sheds further light on the physics underlying this behavior.

III. NUMERICAL RESULTS

Exact soliton solution of the homogeneous version of Eq. (1) is used to start the numerical evolution of the scattering process, namely

$$\psi(x,0) = A\,\frac{\exp\{i\,v_0[x - x_{\text{c.m.}}(0)]\}}{\cosh\{A[x - x_{\text{c.m.}}(0)]\}}, \tag{3}$$

with $A = 1$ and $x_{\text{c.m.}}(0) = x_0$, where v_0 and x_0 are the initial center-of-mass velocity and position, respectively. For the numerical study of the scattering process the initial position of the soliton x_0 is selected to be considerably far from the potential well so there is no interaction between them at $t = 0$. When the soliton is set in motion with initial center-of-mass velocity v_0 and the collision between the soliton and potential arises we may have pure transmission (T), trapping (L), reflection (R), or a combination of these states. The three coefficients must satisfy the conservation law $R + T + L = 1$. These coefficients are determined long after the scattering from the potential well, according to the relations

$$R = \frac{1}{\mathcal{N}}\int_{-\infty}^{-h} |\psi(x)|^2 dx, \quad T = \frac{1}{\mathcal{N}}\int_{h}^{\infty} |\psi(x)|^2 dx,$$
$$L = \frac{1}{\mathcal{N}}\int_{-h}^{h} |\psi(x)|^2 dx, \tag{4}$$

where h denotes a position on the x axis at which the influence of the potential disappears $V(h) \sim 0$, and $\mathcal{N} = \int_{-\infty}^{\infty} |\psi(x)|^2 dx$ is the soliton norm. Notice that the signs of the limits of integrations implicitly assume a negative initial position and a positive initial velocity of the soliton, i.e., incident from left to right. For a soliton incident from right to left, the definitions of R and T should be interchanged.

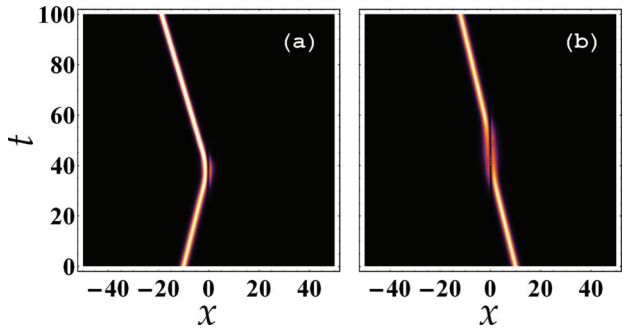

FIG. 1. (Color online) (a) Density plot for a single soliton scattering by a PT-symmetric potential when the soliton is moving from left to right. (b) Same as in (a) but for the motion from right to left. Parameters are as follows: $|v_0| = 0.25$, $|x_0| = 10$, $V_0 = 4$, and $W_0 = 2.0$.

In Fig. 1, the soliton scattered by the PT-symmetric potential is shown with strength $V_0 = 4$, $W_0 = 2$, initial speed $|v_0| = 0.25$, and initial position $|x_0| = 10$. When the soliton collides with the potential moving from the left, it gets reflected completely as in Fig. 1(a), but when the soliton is incident from the right, as in Fig. 1(b), the soliton completely transmits to the other side of the potential. Figure 2 shows the transmission and reflection coefficients as functions of the initial velocity v_0 for a fixed strength of the PT-symmetric potential with $V_0 = 4$ and $W_0 = 2$. Solid and dashed lines indicate the soliton incident from the left and the right, respectively. Figures 2(a) and 2(b) show the remarkable feature that for the incident velocity window $v_0 \in [0.24 - 0.32]$ unidirectional flow takes place. Further details on the dynamics are shown in Figs. 3(a)–3(d), where we plot the amplitude, center-of-mass position, center-of-mass speed, and kinetic energy versus time for both directions of incidence. Figure 3(a) shows amplitude oscillations developing post scattering. These are naturally associated with oscillation in the width of the soliton and, hence, leading to kinetic energy oscillation, as shown in Fig. 3(d).

Figures 3(b) and 3(c) show a reduction in the center-of-mass speed as a result of the scattering. It is also noticed, upon comparing the two curves in each subfigure, that the soliton acquires considerably larger gain in its amplitude and kinetic energy when scattered by the left side of the potential. This asymmetry is inherited from the asymmetry in the imaginary

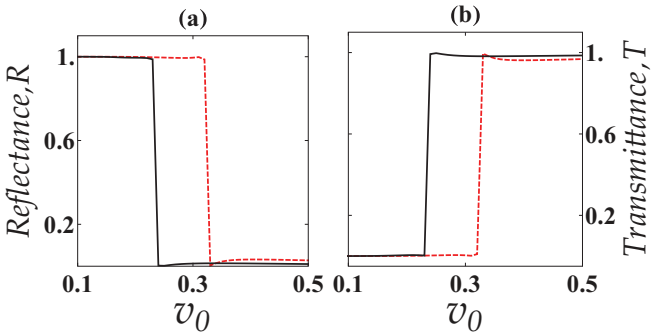

FIG. 2. (Color online) [(a) and (b)] Reflection and transmission coefficients for a soliton moving left (dashed) and right (solid), respectively. Parameters are as follows: $V_0 = 4$, $W_0 = 2$, and $|x_0| = 10$.

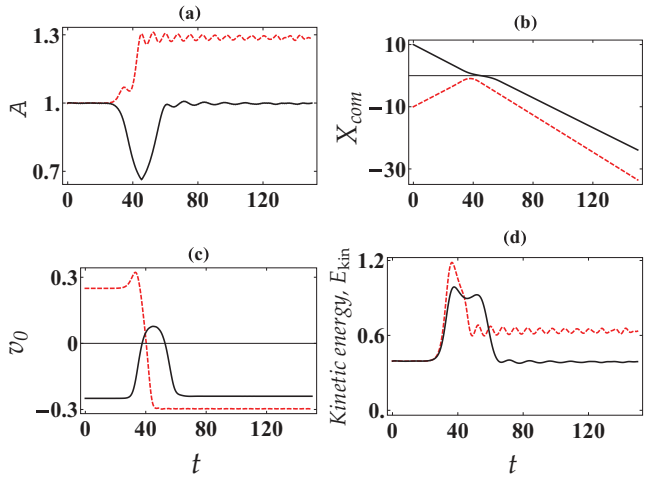

FIG. 3. (Color online) Soliton scattering through a PT-symmetric potential studied numerically by solving the NLS equation: (a) amplitude, (b) center of mass, (c) velocity, and (d) kinetic energy of a soliton moving from left and right (dashed and solid lines, respectively). Parameters are as follows: $V_0 = 4$, $W_0 = 2$, $|x_0| = 10$, and $|v_0| = 0.25$.

part of the potential such that a soliton incident from left will encounter gain [$W(x)$ is negative] and then loss [$W(x)$ is positive] while the situation is reversed for the soliton incident from right. Thus, the outcome of the scattering depends on the order of the sequence of loss and gain regions as encountered by the traveling soliton. The width of the velocity window, Δv, where the unidirectional flow occurs depends on the potential strengths, V_0 and W_0. Figure 4 shows this dependence where it is observed that larger velocity window is obtained with smaller V_0 and larger W_0. That is, in designing such a unidirectional system the dissipative part of the potential plays a constructive role while the real part of the potential is detrimental and should be reduced as much as possible for the realization of this phenomenon.

Finally, the unidirectional flow was also demonstrated for a train of six solitons where the distance between center of masses of adjacent solitons and their initial speed are $|\delta x_0| = 15$ and $|v_0| = 0.25$, respectively, as shown in Fig. 5. Below this value of separation, the scattered solitons start to interact with incident solitons in a manner that destroys the unidirectional flow. In particular, the reflected dispersive wave

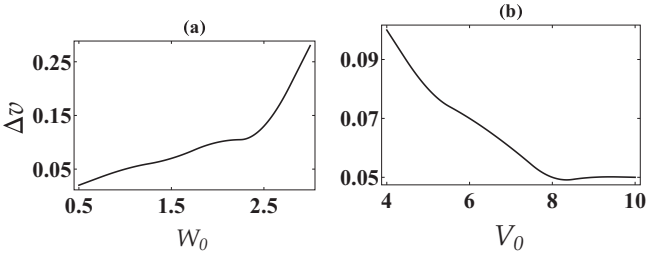

FIG. 4. (a) Velocity window for the unidirectional soliton scattering as a function of W_0 for the strength of real part of the PT-symmetric potential fixed at $V_0 = 4$. (b) Velocity window as a function of V_0 while the strength of imaginary part of PT-symmetric potential is fixed at $W_0 = 2$.

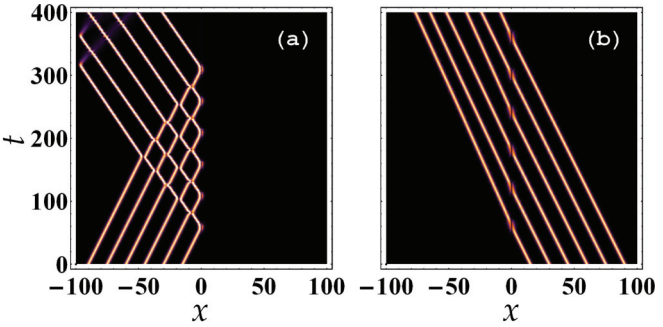

FIG. 5. (Color online) (a) Density plot of a soliton train scattering through a PT-symmetric potential from left to right. (b) Same as in (a) but for the scattering from right to left. Parameters are as follows: $|v_0| = 0.25$, $V_0 = 4$, and $W_0 = 2.5$.

excited from the scattering of one soliton will perturb the profile of adjacent incident soliton and its center-of-mass speed leading to a different outcome than for the unperturbed soliton. For the used values of V_0 and W_0, a minimum separation of 15 guarantees that such perturbations will not affect the unidirectional flow. The potential strength in both cases was fixed with $V_0 = 4$ and $W_0 = 2.5$. In Fig. 5(a), the soliton train was transmitted while in Fig. 5(b) it was reflected. It is noticed that while the amplitude of the transmitted string of solitons is almost equal to that of the incident one, the amplitude of the reflected solitons is almost doubled. This asymmetry is again a consequence of the fact that while in one case the soliton experience gain followed by loss, in the other case the case it experiences loss followed by gain.

IV. COLLECTIVE-COORDINATE APPROACH

The numerical results of the previous section have shed some light on the physics behind the soliton unidirectional flow. The incoming soliton experiences an increase or a decrease in its center-of-mass speed depending on the direction from which it is incident on the PT-symmetric potential. There are two mechanisms by which the PT-symmetric potential changes the center-of-mass speed of the incoming soliton, the first being the mixing of the center-of-mass motion with the internal modes of the soliton such that breathing modes are excited from a reduction in the center-of-mass kinetic energy. This is evident from the oscillations in the amplitude and kinetic energy of the scattered soliton, as shown in Fig. 3 and discussed in the previous section. The second mechanism for center-of-mass speed change is the damping and gain provided by the imaginary part of the PT-symmetric potential. While damping acts on one side of the potential, gain acts on the other. A soliton incident from the damping side will experience a reduction in its center-of-mass speed such that it experiences a quantum reflection from the real part of the potential at the center. On the contrary, a soliton incident from the pumping side will experience an increase in its center-of-mass speed, resulting in a full transmission.

To verify this simple explanation we use in the present section a collective-coordinate approach to derive the equation of motion for the center-of-mass of the soliton. It turns out that the imaginary part of the PT-symmetric potential results in a term that is damping or pumping depending on the direction

of the incoming soliton. For feasibility of calculations, we use a PT-symmetric potential composed of δ functions as follows:

$$V(x) = V_0\,\delta(x), \quad W(x) = W_0\,[\delta(x-L) - \delta(x+L)], \tag{5}$$

which represents a δ-potential well (barrier) at $x = -L(L)$ with strength W_0 and a δ potential well at $x = 0$ with strength V_0. Notice that the potential in Eq. (1) is given by $-V(x) - i\,W(x)$. Clearly, this potential captures the main PT-symmetric features of the original potential in Eq. (2).

Focusing on the dynamics of the center of mass, we employ the following ansatz:

$$\psi(x,t) = \eta \frac{\exp\{-i\mu(t)[x-\xi(t)]\}}{\cosh\{[x-\xi(t)]/\alpha\}}, \tag{6}$$

where $\xi(t)$ and $\mu(t)$ are time-dependent variational parameters corresponding to the center-of-mass position and center-of-mass speed, respectively. The width, α, and amplitude, η, are taken here independent of time. For completeness, we review here briefly the collective-coordinate approach [11].

We start by rewriting the NLS equation in the form

$$i\frac{\partial\psi}{\partial t} = \frac{\delta H_0}{\delta\psi^*} + R[\psi(x,t);x,t], \tag{7}$$

where

$$H_0 = \frac{1}{2}\int_{-\infty}^{+\infty} dx(\psi_x\psi_x^* - \psi^2\psi^{*2}) \tag{8}$$

and

$$R[\psi(x,t);x,t] = -[V(x) + iW(x)]\psi. \tag{9}$$

By assuming $\psi(x,t)$ and its conjugate to vary with time via a set of time-dependent variational parameters, $\overrightarrow{Y}(t) := \{\eta(t),\xi(t),\mu(t),\alpha(t),\beta(t),\phi(t)\}$, the equations of motion for the variational parameters can be derived from the relations

$$\sum_{j=1}^{6} I_{Y_nY_j}\dot{Y}_j = F_n(\overrightarrow{Y}) + R_n(\overrightarrow{Y}), \quad n = 1,2,\ldots 6, \tag{10}$$

with

$$I_{Y_nY_j} = i\int_{-\infty}^{+\infty} dx\left(\frac{\partial\psi}{\partial Y_n}\frac{\partial\psi^*}{\partial Y_j} - \frac{\partial\psi^*}{\partial Y_n}\frac{\partial\psi}{\partial Y_j}\right), \tag{11}$$

$$F_n(\overrightarrow{Y}) = -\frac{\partial H_0}{\partial Y_n}, \tag{12}$$

$$R_n(\overrightarrow{Y}) = -\int_{-\infty}^{+\infty} dx\left(R\frac{\partial\psi^*}{\partial Y_n} + R^*\frac{\partial\psi}{\partial Y_n}\right), \tag{13}$$

where the dot denotes the derivative with respect to time.

The equations of motion for $\xi(t)$ and $\mu(t)$ read

$$\dot{\xi}(t) = -\mu(t) + \frac{W_0}{\alpha}\left\{[L-\xi(t)]\,\mathrm{sech}^2\left[\frac{L-\xi(t)}{\alpha}\right] + [L+\xi(t)]\,\mathrm{sech}^2\left[\frac{L+\xi(t)}{\alpha}\right]\right\}, \tag{14}$$

$$\dot{\mu}(t) = -\frac{V_0}{2\alpha}\frac{d}{d\xi(t)}\mathrm{sech}^2\left[\frac{\xi(t)}{\alpha}\right] - \frac{W_0}{a}\left\{\mathrm{sech}^2\left[\frac{L+\xi(t)}{\alpha}\right] - \mathrm{sech}^2\left[\frac{L-\xi(t)}{\alpha}\right]\right\}\mu(t). \tag{15}$$

Eliminating $\mu(t)$, the following equation of motion for $\xi(t)$ is obtained:

$$\ddot{\xi} + \Gamma[\xi]\,\dot{\xi} + f[\xi] = 0, \tag{16}$$

where

$$\Gamma[\xi] = \frac{2W_0}{\alpha^2}\left[(L+\xi)\,\mathrm{sech}^2\left(\frac{L+\xi}{\alpha}\right)\tanh\left(\frac{L+\xi}{\alpha}\right) - (L-\xi)\,\mathrm{sech}^2\left(\frac{L+\xi}{\alpha}\right)\tanh\left(\frac{L+\xi}{\alpha}\right)\right] \tag{17}$$

and

$$f[\xi] = V_0\,\mathrm{sech}^2\left(\frac{\xi}{\alpha}\right)\tanh\left(\frac{\xi}{\alpha}\right) - \frac{W_0^2}{\alpha^2}\left[\mathrm{sech}^2\left(\frac{L+\xi}{\alpha}\right) - \mathrm{sech}^2\left(\frac{L-\xi}{\alpha}\right)\right]^2\xi - \frac{W_0^2}{\alpha^2}\left[\mathrm{sech}^4\left(\frac{L+\xi}{\alpha}\right) - \mathrm{sech}^4\left(\frac{L-\xi}{\alpha}\right)\right]L. \tag{18}$$

The center-of-mass equation of motion is, thus, similar to that of a classical particle subject to a velocity-dependent damping/gain force, $\Gamma[\xi]\,\dot{\xi}$, and a position-dependent effective force, $-f[\xi]$. The sign of the position-dependent damping or gain coefficient determines weather the soliton will be subject to damping or gain such that for $\Gamma[\xi] > 0 (< 0)$, the soliton will be subject to damping (gain). Plotting $f[\xi]$ and $\Gamma[\xi]$ versus ξ shows that a soliton incident from the left (right) will be subject to damping (gain), as shown in Fig. 6. This verifies the above-mentioned asymmetry in damping and gain. Since the peaks of damping (gain) is off-centered, the velocity reduction (increase) takes place before the soliton reaches the potential well at the center and thus reflects (transmits).

To estimate the velocity reduction caused by the damping part on a soliton incoming from the left, we neglect in Eq. (16) the terms originating from the δ function on the right, namely those with $L-\xi$ but keeping the terms with $L+\xi$. In addition, we assume, for simplicity, weak damping so we can neglect terms proportional to W_0^2. Since the real part of the potential is symmetric we also ignore the V_0 term in order to focus on the asymmetric imaginary part of the potential. The equation

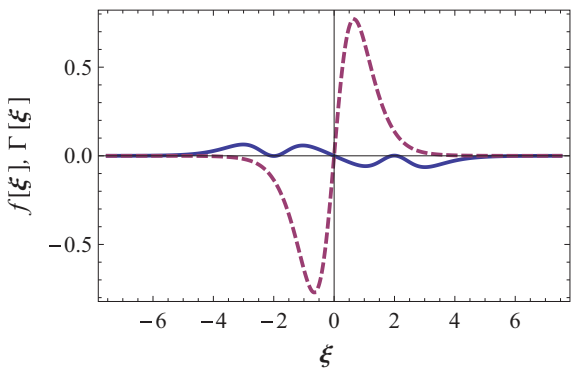

FIG. 6. (Color online) Effective force, $-f[\xi]$, shown with dashed curve and damping rate, $\Gamma[\xi]$, shown with solid curve. the curves are given by Eqs. (17) and (18). Parameters are as follows: $\alpha = \eta = 1$, $V_0 = 2$, $L = 2$, and $W_0 = 0.1$.

of motion then simplifies to

$$\ddot{\xi} + \frac{2W_0}{\alpha^2}(L+\xi)\,\mathrm{sech}^2\left(\frac{L+\xi}{\alpha}\right)\tanh\left(\frac{L+\xi}{\alpha}\right)\dot{\xi} = 0, \tag{19}$$

which can be written as

$$\ddot{\xi} + \frac{W_0}{\alpha}\frac{d}{dt}\left[\alpha\tanh\left(\frac{L+\xi}{\alpha}\right) - (L+\xi)\,\mathrm{sech}^2\left(\frac{L+\xi}{\alpha}\right)\right] = 0. \tag{20}$$

Integrating, we obtain

$$\dot{\xi} = v_0 - W_0 - \frac{W_0}{\alpha}\left[\alpha\tanh\left(\frac{L+\xi}{\alpha}\right) - (L+\xi)\,\mathrm{sech}^2\left(\frac{L+\xi}{\alpha}\right)\right], \tag{21}$$

where the initial condition $\dot{\xi}(-\infty) = v_0$ is satisfied by substituting $\xi(-\infty) = -\infty$ in the previous equation. Assuming $\xi(0) = 0$, the velocity reduction thus can be calculated as

$$\begin{aligned}\Delta v &\equiv \dot{\xi}(0) - \dot{\xi}(-\infty)\\ &= -W_0 - \frac{W_0}{\alpha}\left[\alpha\tanh\left(\frac{L}{\alpha}\right) - L\,\mathrm{sech}^2\left(\frac{L}{\alpha}\right)\right],\end{aligned} \tag{22}$$

which is identically negative. Clearly, a soliton incident from the right direction will experience velocity increase that is equal to $|\Delta v|$.

Finally, we note that while the collective-coordinate approach provides a general theoretical explanation for the existence of the unidirectional flow, a direct comparison of its predicted dynamics with the numerical solution of the NLS equation is not performed for two main reasons. First, the profiles of the PT-symmetric potentials, Eqs. (2) and (5), are different. Second, the collective-coordinate approach is an approximate calculation so no quantitative agreements with the direct numerical simulations of the soliton directional flow is expected.

V. CONCLUSIONS

We have predicted and demonstrated numerically the effect of unidirectional soliton flows for the PT-symmetric potentials. We have observed that almost perfect transmission of solitons takes place in one direction and almost perfect reflection occurs in the other direction. We believe that the asymmetry in the sequence of pumping and damping is essentially the main reason for this behavior. In addition, an internal mode is excited at the expense of the center-of-mass kinetic energy. Both effects cause a velocity reduction that may or may not lead to the soliton transmission through the potential. If, for example, the soliton propagates from the right, it encounters, first, the gain region accompanied by some velocity increase that keeps its speed above the critical value for reflection, as a result, the soliton transmits. On the other hand, in the same system the soliton scattering from the left will first encounter the lossy region accompanied by a velocity reduction. Here, the soliton velocity will reduce becoming lower than the critical velocity for reflection, and, hence, the soliton will be reflected.

This mechanism has been verified by studying the excitation of the soliton internal mode and the velocity reduction as shown in Fig. 3. Furthermore, a collective-coordinate approach has verified qualitatively that the soliton experiences an asymmetric position-dependent damping. Finally, the unidirectional flow was also demonstrated for the multisoliton case. Almost perfect unidirectional flow was also obtained but under the requirement of well-separated solitons.

ACKNOWLEDGMENTS

The authors acknowledge the support of the King Fahd University of Petroleum and Minerals (under Projects No. RG1217-1 and No. RG1217-2), the Saudi Center for Theoretical Physics (SCTP), and a UAEU-NRF research grant.

[1] C. M. Bender and S. Boettcher, Phys. Rev. Lett. **80**, 5243 (1998); C. M. Bender, S. Boettcher, and P. N. Meisinger, J. Math. Phys. **40**, 2201 (2001); C. M. Bender, P. N. Meisinger, and Q. Wang, J. Phys. A: Math. Gen. **36**, 1973 (2003); C. M. Bender, M. V. Berry, and A. Mandilara, *ibid.* **35**, L467 (2002); C. M. Bender, D. C. Brody, and H. F. Jones, Phys. Rev. D **70**, 025001 (2004).

[2] R. El-Ganainy, K. G. Makris, D. N. Christodoulides, and Z. H. Musslimani, Opt. Lett. **32**, 2632 (2007); A. Regensburger, C. Bersch, M. Miri, G. Onishchukov, D. N. Christodoulides, and U. Peschel, Nature **488**, 167 (2012); C. E. Rutter, K. G. Makris, R. El-Ganainy, D. N. Christodoulides, M. Segev, and D. Kip, Nat. Phys. **6**, 192 (2010); K. G. Makris, R. El-Ganainy, D. N. Christodoulides, and Z. H. Musslimani, Phys. Rev. Lett. **100**, 103904 (2008); Z. H. Musslimani, K. G. Makris, R. El-Ganainy, and D. N. Christodoulides, *ibid.* **100**, 030402 (2008); M. V. Berry, J. Phys. A **41**, 244007 (2008); S. Longhi, Phys. Rev. Lett. **103**, 123601 (2009); Y. V. Kartashov *et al.*, Opt. Lett. **35**, 1638 (2010); C. T. West, T. Kottos, and T. Prosen, Phys. Rev. Lett. **104**, 054102 (2010); S. Longhi, Phys. Rev. B **80**, 235102 (2009); O. Bendix, R. Fleischmann, T. Kottos, and B. Shapiro, Phys. Rev. Lett. **103**, 030402 (2009); S. Klaiman, U. Gunther, and N. Moiseyev, *ibid.* **101**, 080402 (2008).

[3] Z. H. Musslimani, K. G. Makris, R. El-Ganainy, and D. N. Christodoulides, J. Phys. A **41**, 244019 (2008).

[4] S. Hu, X. Ma, D. Lu, Z. Yang, Y. Zheng, and W. Hu, Phys. Rev. A **84**, 043818 (2011); S. Hu and W. Hu, J. Phys. B **45**, 225401 (2012); A. Khare, S. M. Al-Marzoug, and H. Bahlouli, Phys. Lett. A **376**, 2880 (2012); D. A. Zezyulin and V. V. Konotop, Phys. Rev. A **85**, 043840 (2012).

[5] E. N. Tsoya, S. Tadjimuratova, and F. Kh. Abdullaev, Opt. Commun. **285**, 3441 (2012).

[6] N. V. Alexeeva, I. V. Barashenkov, A. A. Sukhorukov, and Yu. S. Kivshar, Phys. Rev. A **85**, 063837 (2012); R. Driben and B. A. Malomed, Opt. Lett. **36**, 4323 (2011).

[7] R. H. Goodman, P. Holmes, and M. I. Weinstein, Physica D **192**, 215 (2004); H. Sakaguchi and M. Tamura, J. Phys. Soc. Jpn. **73**, 503 (2004).

[8] S. V. Dmitriev, S. V. Suchkov, A. A. Sukhorukov, and Yu. S. Kivshar, Phys. Rev. A **84**, 013833 (2011).

[9] L. Feng, Ye-Long Xu, W. S. Fegadolli, Ming-Hui Lu, J. E. B. Oliveira, V. R. Almeida, Yan-Feng Chen, and A. Scherer, Nature Mat. 12 (2013).

[10] C. Lee and J. Brand, Europhys. Lett. **73**, 321 (2006).

[11] Niurka R. Quintero, Franz G. Mertens, and A. R. Bishop, Phys. Rev. E **82**, 016606 (2010).